Supplementary Information

Copper clusters as novel fluorescence probes for lead ions detection and their photocatalytic elimination

Noelia Vilar-Vidal[∫,†], José Rivas Rey[∫,†], M.A. López Quintela†.

†Nanomag Laboratory, Research Technological Institute, University of Santiago de Compostela, E-15782, Santiago de Compostela, Spain

[∫]INL – International Iberian Nanotechnology Laboratory, 4715-310 Braga, Portugal

*Corresponding Author Email: malopez.quintela@usc.es

Contents:

M) **Schematic energy diagram showing the Hg^{+2} detection by different Au protected clusters (Figure S11).**

N) **Schematic energy diagram showing the Pb^{+2} detection by different Cu protected clusters and Au-MUA protected clusters (Figure S12).**

O) **2D cation effect diagram on the PL intensity for the small (Cu_7) and large (Cu_{20}) CLs (Figure S13).**

P) Cation effect (4ppm) on the Cu_7CLs PL intensity (Figure S14).

Q) Cation effect (4ppm) on the Cu_{20}CLs PL intensity (Figure S15).

R) Schematic energy diagram showing the different CuCLs sizes (HOMO/LUMO) vs ion redox potentials (Figure S16).

Experimental Section

Chemicals: All chemicals were of analytical grade and were used without further purification. The water used in all experiments was mili-Q grade. Tetrabutylammonium acetate (99%, Fluka), acetonitrile (99,9%, Sigma-Aldrich), Copper electrode (99.99%, GoodFellow), Platinum electrode (99.95%, GoodFellow), Aluminium oxide (99.99%, Alfa Aesar), Sulfuric acid (97%, Merck), Tetrabutylammonium nitrate (>97%, Fluka), ethanol (99.99%, GPR-Rectapur), Copper nitrate (98%, Sigma-Aldrich), Lead nitrate (99%, Sigma-Aldrich), Ferric nitrate (98%, Panreac), Zinc Sulphate (99%, Sigma-Aldrich), Potasium hydroxide (Sigma-Aldrich), Nickel nitrate (Sigma-Aldrich), Aluminium nitrate (99%, Sigma-Aldrich).

Synthesis of Copper Clusters: Copper clusters were electrochemically synthesized using an Autolab PGSTAT 20 potenciostat by a slight modification of previous reported protocols.[1] Summarizing, the synthesis have been performed in a thermostatic three-electrode electrochemical cell. For the medium CuCLs (13 atoms clusters) tetrabutylammonium nitrate (0.1M in water) was used as the supporting electrolyte and capping agent. A copper sheet was used as an anode (counter electrode) and the same size platinum as a cathode (working electrode). An Ag/AgCl electrode was used as reference. Both the working (Pt) and the counter electrode (Cu) were carefully cleaned before synthesis; the Pt electrode was mirror-like polished with aluminium oxide, and the copper electrode cleaned with sandpaper. Both electrodes were then washed with water in an ultrasonic bath. Further electrochemical polishing was carried out on the Pt electrode by repeated cyclic voltammetries in 1M sulphuric acid. The cell was maintained under a nitrogen atmosphere and magnetic stirring, keeping the temperature at 25.0 ± 0.1 ºC throughout the whole process. Copper ions produced from the anode electrodissolution were reduced in galvanostatic conditions under 10mA/cm^2 current density during 800 s. Small and large CuCLs (Cu_7 and Cu_{20} clusters) were obtained after a purification and post-treatment procedure, respectively.[1b] Cu_7CLs was obtained after a purification process of the precipitate obtained in the electrochemical synthesis, and centrifuging it in EtOH. On the other hand, Cu_{20}CLs was obtained by a temperature control growth of the on a rotary evaporator at 80ºC and redispersing it in acetonitrile by vigorously stirring for 180 minutes.

Sample Characterization: Synthesized copper clusters were characterized by UV-Vis spectrophotometry using a Hewlett-Packard 8452A Diode Array spectrophotometer (190-800 nm). A 0.1M solution of tetrabutylamonium acetate in acetonitrile was used as a blank. Photoluminescence spectra (200-800 nm) were acquired with a Cary Eclipse Varian at room temperature.

Selectivity Measurements. The following cations were used for the selectivity experiments: nickel, zinc, lead, iron, copper, aluminum and potassium. A 10 mM salt stock solution was prepared and from which the 20μM ion solutions were prepared. The [Cu] in the samples (Cu_7, Cu_{13} and Cu_{20}) is 18μM. Subsequently, salt were prepared from the stock solution by serial dilution.

Sensitivity Measurements. Lead nitrate was used for the Pb^{2+} sensitivity studies. Various Pb^{2+} ion concentrations (0, 0.048 μM, 4.8 μM, 12 μM, 19 μM, 29 μM, 38 μM, 58 μM and 77 μM) were prepared using serial dilution of the lead nitrate stock solution to test the sensitivity limits of the medium size (Cu_{13}) CLs. The [Cu] in the sample is 68μM.

UV irradiation Experiments: Experiments in solution consisted of an aqueous solution of the Pb^{+2} ion (77μM) with Cu_{13} CLs (20μM) by using a fluorescence quartz cuvette. The sample was irradiated under UV light by using a 254nm wavelength UPV pen Ray model 11SC-1 located about 10 cm away from the sample in a closed box with a stable temperature of 30ºC.

A) Schematic representation of copper clusters used in the present study.

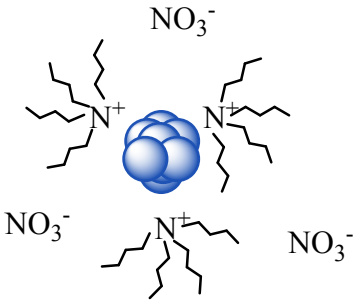

Fig. S 1| Schematic representation of copper clusters protected by $TBANO_3$ (tetrabutylammonium nitrate).

B) PL properties of the different CuCLs sizes used in this study.

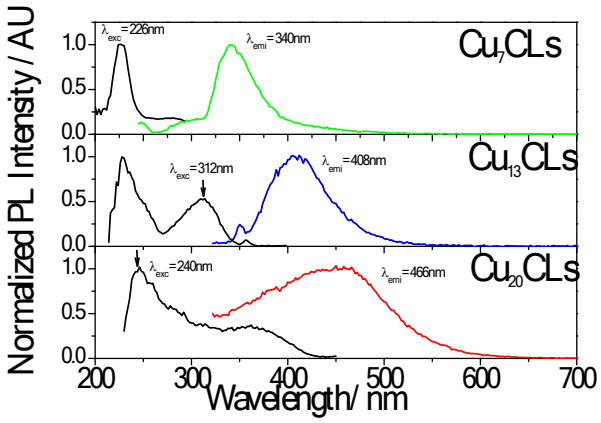

Fig. S2| Excitation/emission scans of different CuCLs sizes. From top to bottom: Cu_7CLs, Cu_{13}CLs and Cu_{20}CLs.

C) Summary of the PL properties of the different CuCLs, their sizes calculed by Jellium and the conduction band (CB) and valence band (VB) position of each one.

Table S1| PL properties of the CuCLs.

CuCLs	Jellium approximation(N) $Eg = AN^{-1/3}$	λ_{exc}[nm]/E[eV]	λ_{emi}[nm]/ E[eV]	CB[eV]	VB[eV]
Cu_7	7	226/5.49	340/3.65	-3.5	-8.6
Cu_{13}	13	312/3.97	408/3.04	-4.5	-8
Cu_{20}	20	240/5.16	466/2.66	-5.5	-7.7

D) (NC-AFM) images of the different types of CuCLs .

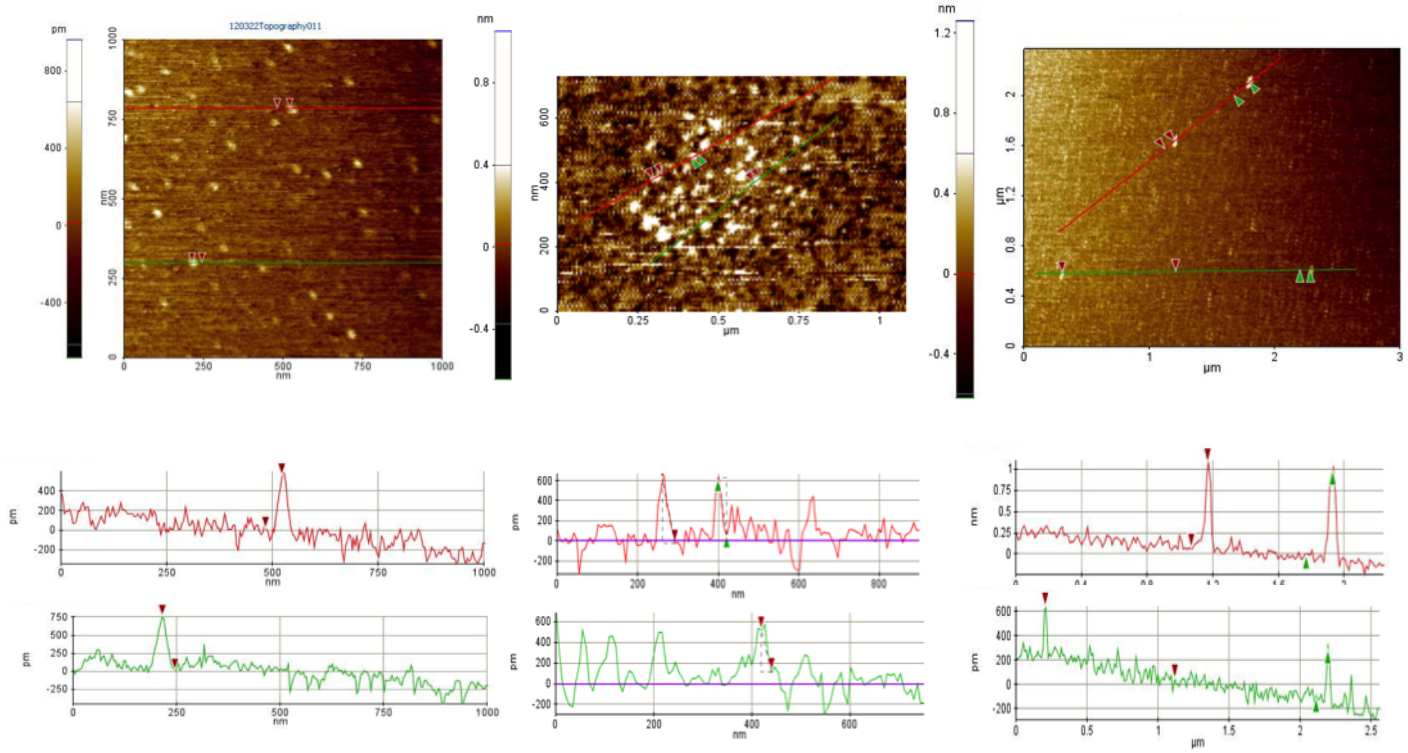

Average height	0.49±0.23nm	0.65±0.27nm	0.98±0.41nm

Fig. S3| NC-AFM topography images of CuCLs (of different sizes) deposited on mica substrates (rms≈150pm): Cu_7, Cu_{13}, and Cu_{20} (top). Section analysis of the solid lines of AFM images (bottom) and their corresponding average heights.

E) Photobleaching study of the different CuCLs sizes.

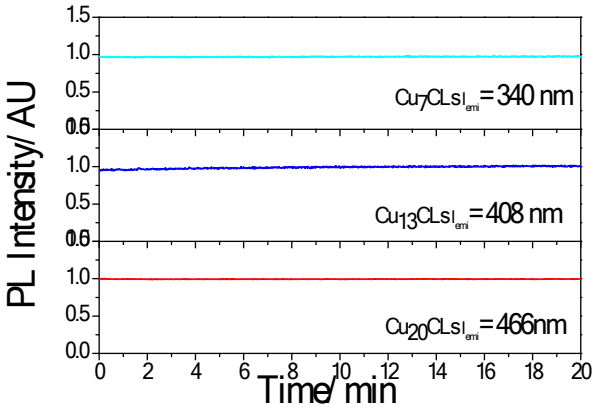

Fig. S 4| Photobleaching study of CuCLs of different sizes during irradiation time of 20 minutes. Collection time for each point 1s.

F) 2D cation effect diagram on the Cu_{13}CLs PL intensity.

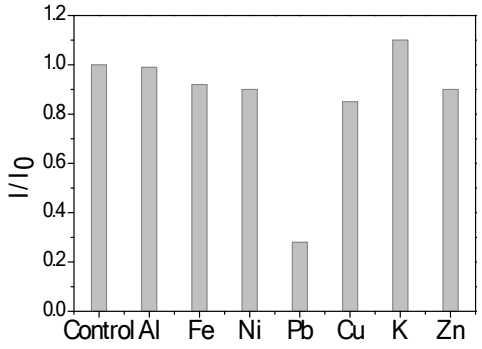

Fig. S 5| 2D Bar diagram showing the effect of different ions (20μM) on the PL intensity of the Cu_{13} CLs in aqueous solution (λ_{emi}=408nm).

G) Cation effect (1ppm) on the Cu_{13}CLs PL intensity.

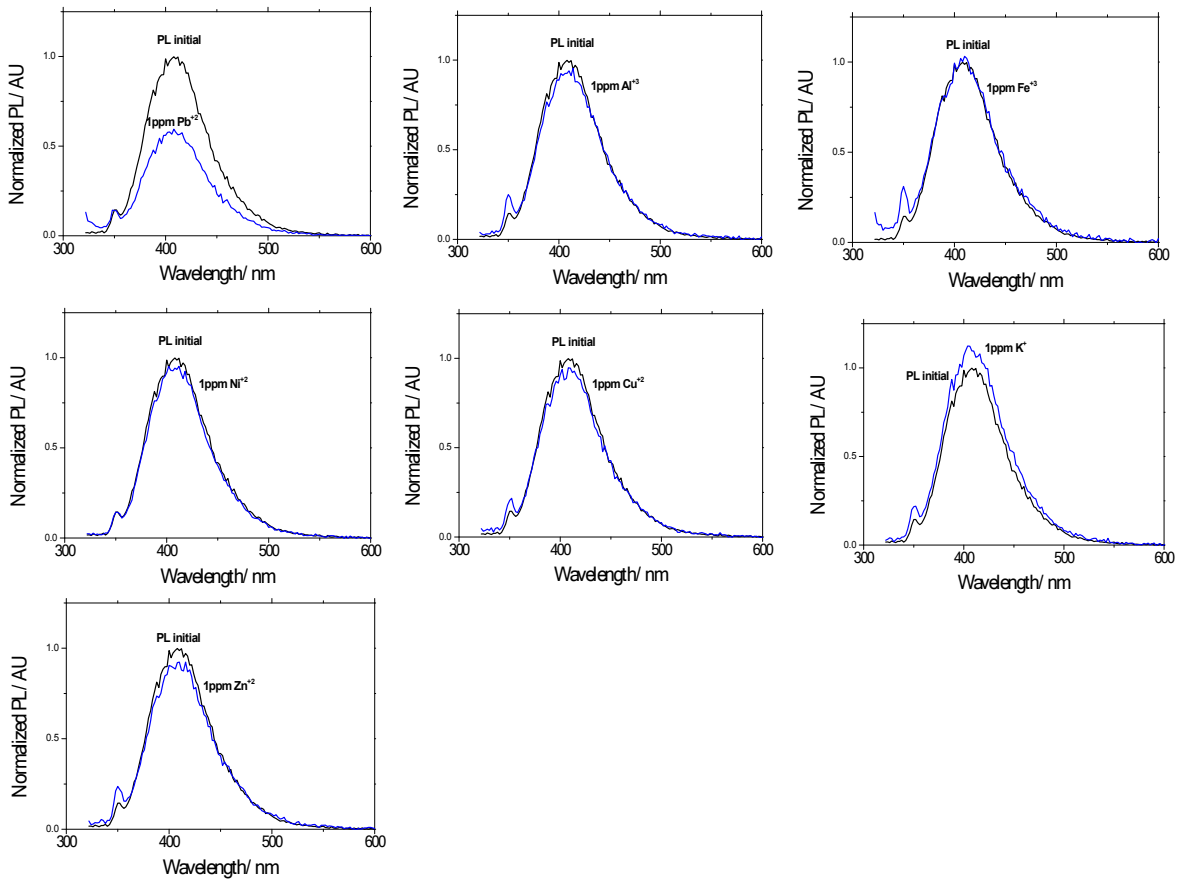

Fig. S 6|Normalized PL intensity of Cu_{13} CLs in presence of 1ppm of different cations: Pb^{+2}, Al^{+3}, Fe^{+3}, Ni^{+2}, Cu^{+2}, K^{+} and Zn^{+2}.

H) 3D Pb^{+2} effect diagram on the Cu_{13}CLs PL intensity.

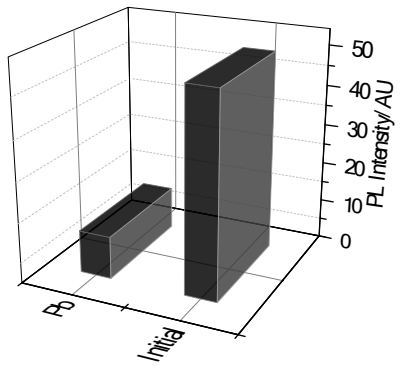

Fig. S 7| Sensitivity of the fluorescence of Cu_{13} CLs towards Pb^{+2} (20μM) in aqueous solutions.

I) Pb^{+2} LOD of by fluorescent Cu_{13}CLs.

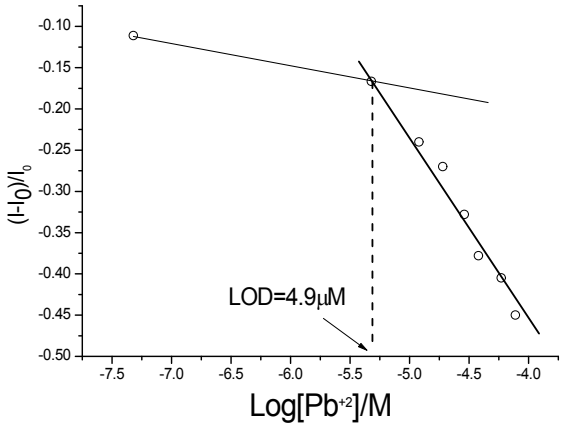

Fig. S8|$I-I_0/I_0$ vs Log $[Pb^{+2}]$/ M plot where I_0 indicates the initial fluorescence intensity of the Cu_{13} CLs and I represent the fluorescence intensity after the addition of a measured amount of Pb^{+2} ions. LOD represents the lower detection limit

I) Literature review of metal clusters used as fluorescent nanoprobes.

Table S2: Experimental conditions and mechanism propose for the different metal ion detections by fluorescent metal clusters literature.

Cluster	Protecting Ligand*	Ion Detected	Redox Potential/V	E*/eV	BG/eV	HOMO/eV	LUMO/ eV	Mechanism	Redox Works	Ref.
Au	Lys	Cu^{+2}	+0.34	-4.75	2.97	-6.985	-4.015	-COOH coordination	Yes	2
Au	DTT	Cu^{+2}	+0.34	-4.75	2.053	-6.53	-4.47	-SH or –OH coordination	Yes	3
Ag	PMAA	Cu^{+2}	+0.34	-4.75	2.02	-6.5	-4.49	-COOH coordination	Yes	4
Ag	DNA	Cu^{+2}	+0.34	-4.75	2.17	-6.585	-4.415	-	Yes	5
Au/Ag	HSA	Cu^{+2}/ Hg^{+2}	+0.34/+0.92	-4.75/-5.4	1.999	-6.5	-4.5	Energy transfer	Yes	6
Ag	PMAA	Cu^{+2}/ Hg^{+2}	+0.34/+0.92	-4.75/-5.4	2.03	-6.51	-4.48	-	Yes	7
Au	1-DOPA	Fe^{+3}	+0.77	-5.2	2.36	-6.68	-4.32	COOH	Yes	8
Au	-	Hg^{+2}	0.92	-5.4	1.94	-6.47	-4.53	metallophilic bonding		9
Ag	LA	Hg^{+2}	0.92	-5.4	1.9	-6.45	-4.54	-COOH coordination	Yes	10
Au	BSA	Hg^{+2}	0.92	-5.4	1.9	-6.45	-4.54	Hg–S bond	Yes	11
Au	Lysoz	Hg^{+2}	0.92	-5.4	2.88	-6.94	-4.06	-	Yes	12
					1.88	-6.44	-4.55			
	BSA	Hg^{+2}	0.92	-5.4	1.94	-6.47	-4.53		Yes	
Au	MUA	Hg^{+2}	0.92	-5.4	2.38	-6.69	-4.3	-COOH coordination	Yes	13
Cu	BSA	Pb^{+2}	-0.13	-4.4	3.04	-8.52	-5.48	-COOH coordination	Yes	14
Au	MUA	Pb^{+2}	-0.13	-4.4	2.44	-6.72	-4.28	-COOH coordination	Yes	15

* Lys (lysine), DTT (Dithiothreitol), PMAA Poly(methacrylic acid), HSA(Human serum albumin), Poly(methacrylic acid sodium salt) (PMAA), l-3,4-dihydroxyphenylalanine (l-DOPA), LA (Lipoic acid), BSA(Bovine serum albumin),Lisoz (Lysozime), MUA (Mercaptoundecanoic acid).

J) Schematic energy diagram showing the Cu^{+2} detection by different Au and Ag protected clusters with lysine (Lys), dodecanethiol (DDT), human serum albumin (HSA), poly(methacrylic acid) (PMAA) and DNA.

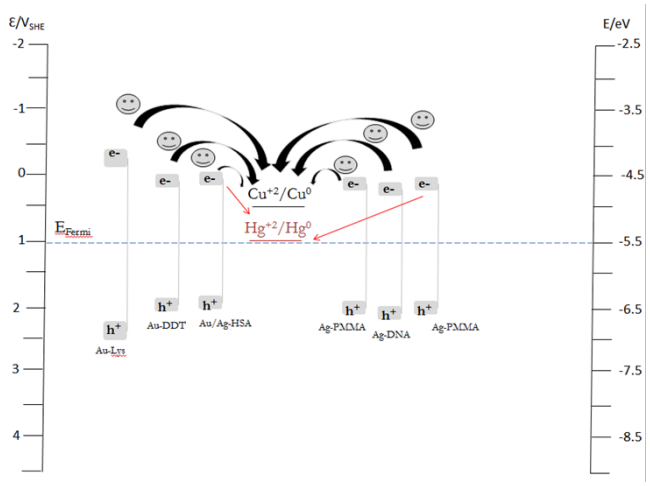

Fig. S 9| Schematic energy diagram showing the Cu^{+2} detection using Au-Lys clusters[2] , Au-DDT clusters[3] , Ag-PMMA clusters[4] , Ag-DNA clusters[5] and Au/Ag-HSA clusters[6] by the probability of the e^- transfer mechanism.

K) Schematic energy diagram showing the Fe^{+3} detection by Au l-3,4-dihydroxyphenylalanine (l-DOPA) protected clusters.

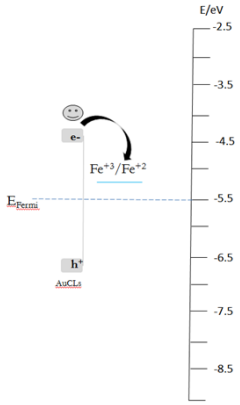

Fig. S 10| Schematic energy diagram showing the Fe^{+3} detection by using Au clusters[8] , by the probability of the e^- transfer mechanism.

L) Schematic energy diagram showing the Hg^{+2} detection by different Au protected clusters.

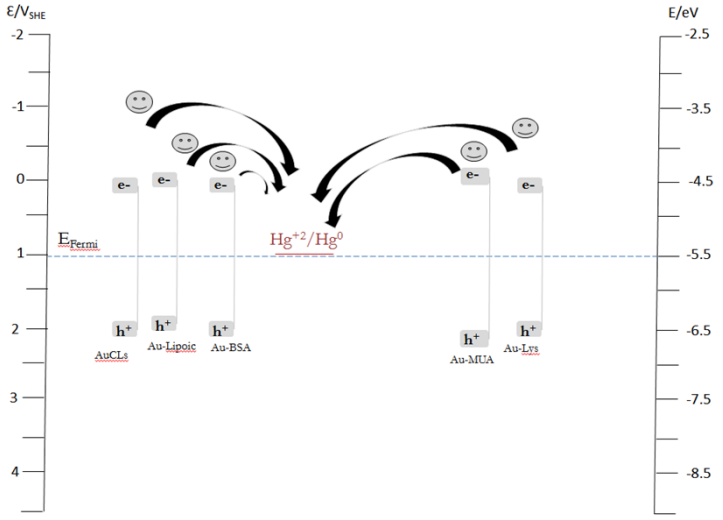

Fig. S11| Schematic energy diagram showing the Hg^{+2} detection by using Au clusters[9] , Au-Lipoic clusters,[10] Au-BSA clusters,[11] Au-Lys clusters[12] and Au-MUA clusters[13] by the probability of the e^- transfer mechanism.

M) Schematic energy diagram showing the Pb^{+2} detection by different Cu protected clusters and Au-MUA protected clusters.

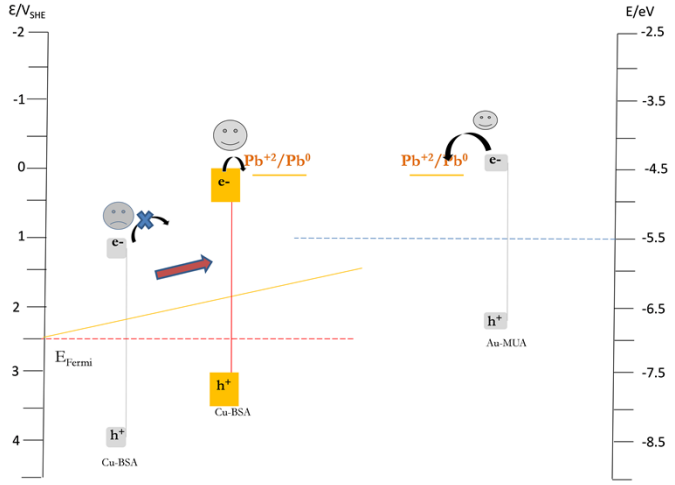

Fig. S 12| Schematic energy diagram showing the Pb^{+2} detection by using Cu BSA clusters[14] and Au-MUA clusters,[15] by the probability of the e^- transfer mechanism.

N) 2D cation effect diagram on the PL intensity for the small (Cu_7) and large (Cu_{20}) CLs.

A) **B)**

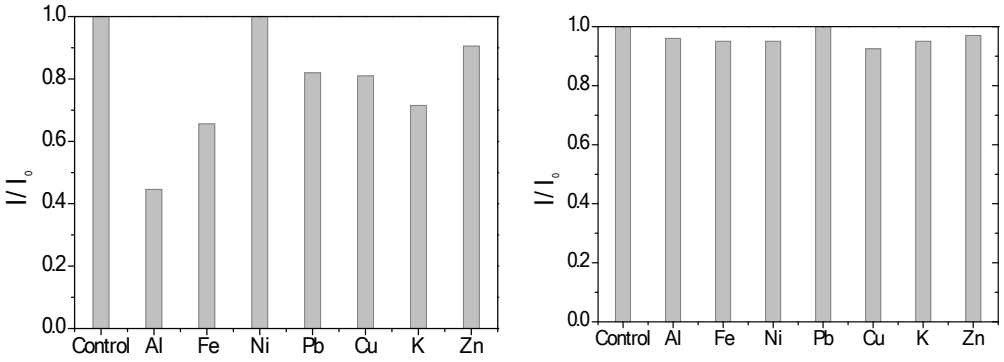

Fig. S13|(A) 2D Bar diagram showing the effect of different ions (4ppm) on the fluorescence of the Cu_7 CLs in aqueous solution (λ_{emi}=340nm). (B) 2D Bar diagram showing the effect of different ions (4ppm) on the fluorescence of the Cu_{20} CLs in aqueous solution (λ_{emi}=466nm).

O) Cation effect (4ppm) on the Cu_7CLs PL intensity.

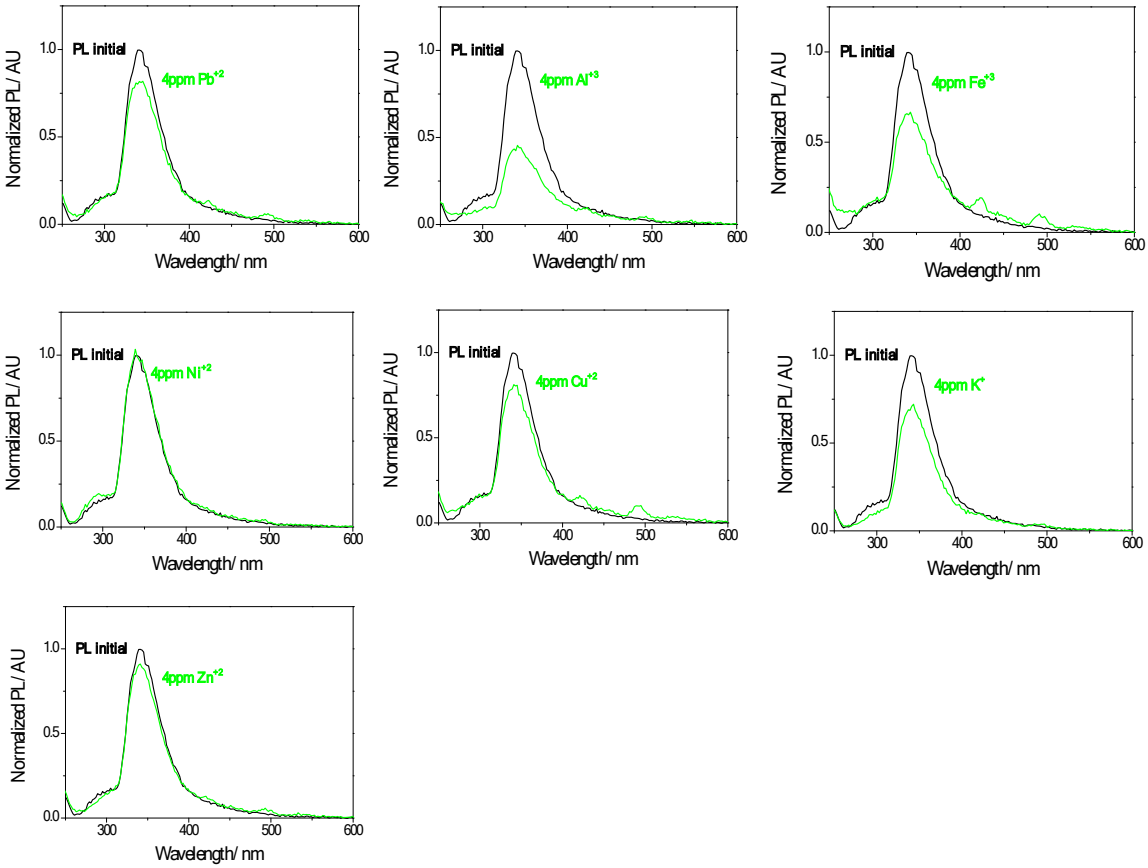

Fig. S14|Normalized PL intensity of the Cu_7 CLs in presence of 4ppm of different ions: Pb^{+2}, Al^{+3}, Fe^{+3}, Ni^{+2}, Cu^{+2}, K^{+} and Zn^{+2}.

P) Cation effect (4ppm) on the Cu_{20}CLs PL intensity.

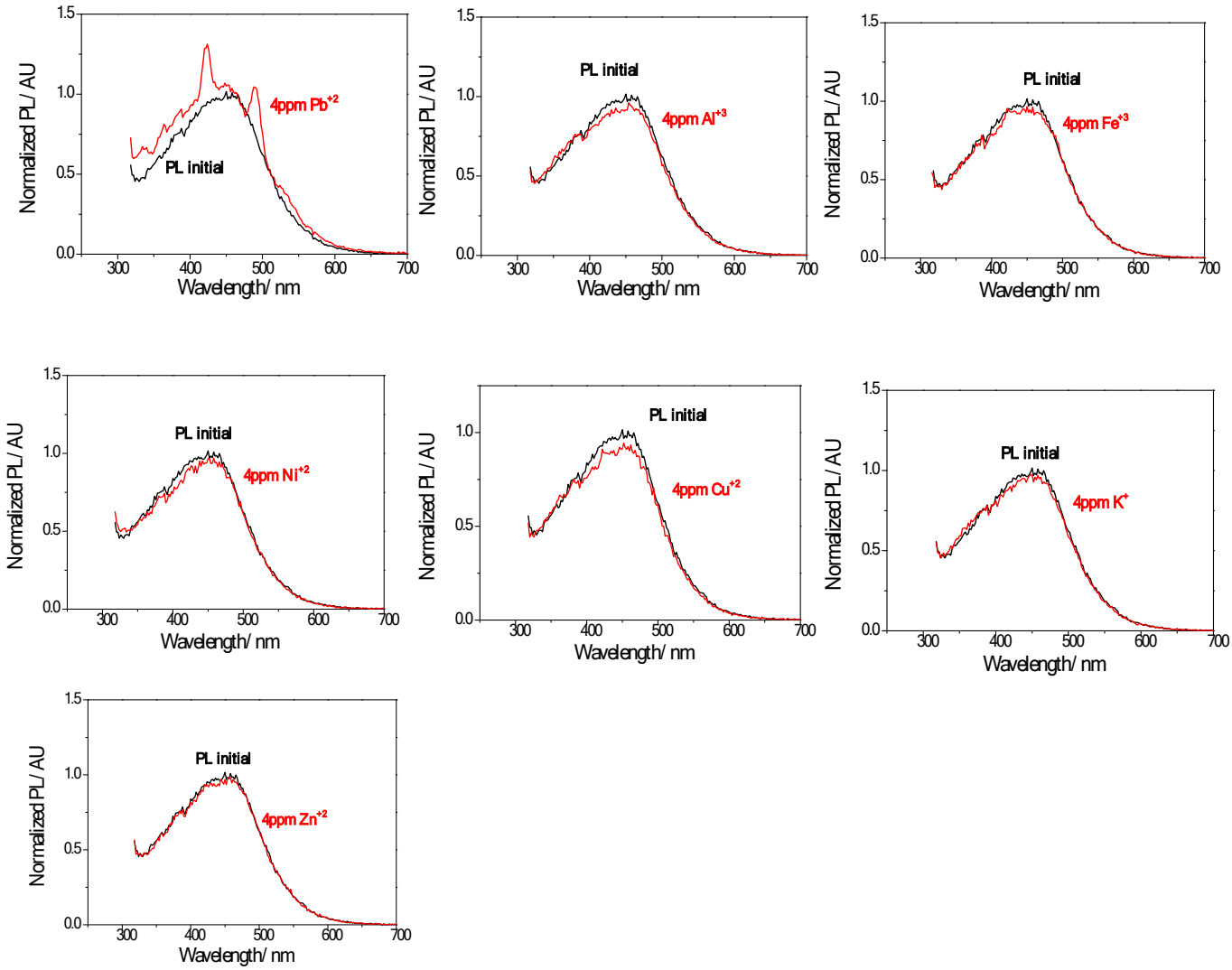

Fig. S15|Normalized PL intensity of the Cu_{20} CLs in presence of 4ppm of different ions: Pb^{+2}, Al^{+3}, Fe^{+3}, Ni^{+2}, Cu^{+2}, K^{+} and Zn^{+2}.

Q) Schematic energy diagram showing the different CuCLs sizes (HOMO/LUMO) vs ion redox potentials.

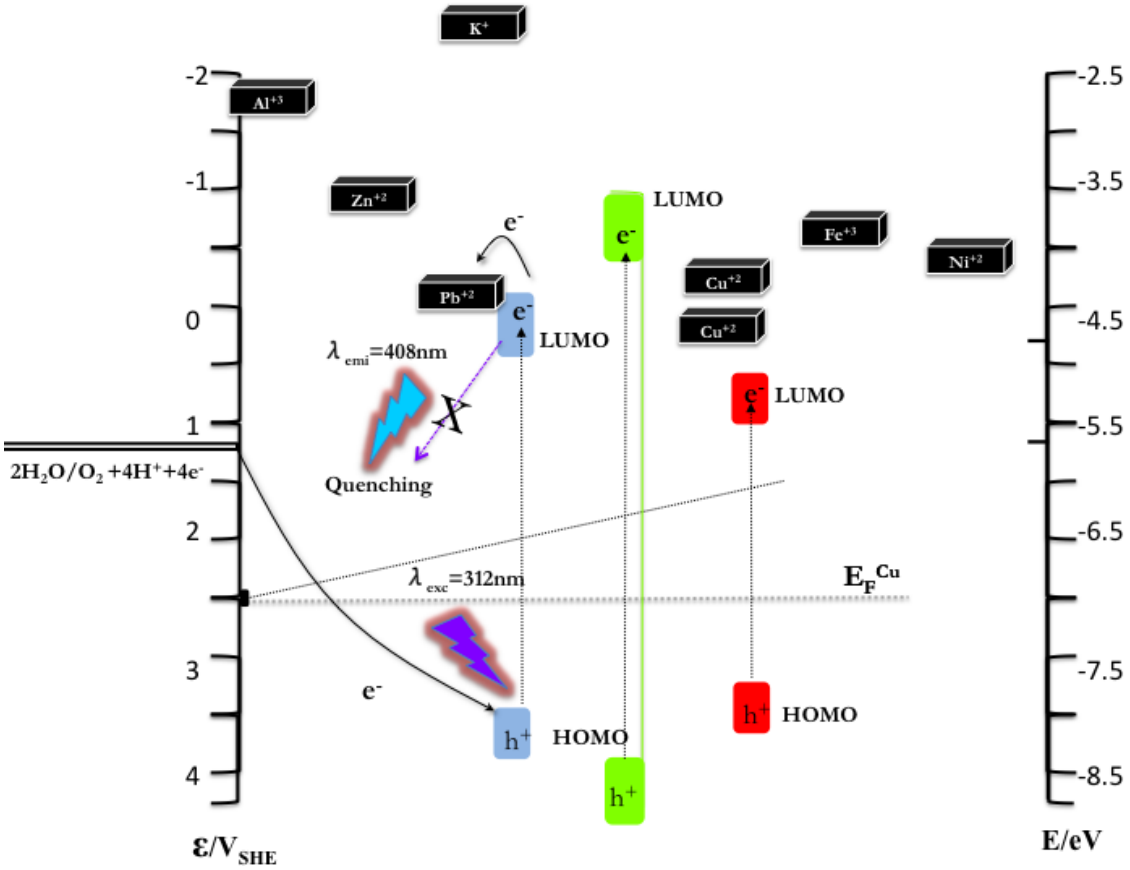

Fig. S16|Schematic Diagram of the HOMO/LUMO position for the different CuCLs sizes and the representation of the ion redox potentials.

---

[1] a) N. Vilar-Vidal, M.C. Blanco, M. A. López-Quintela, J. Rivas, C. Serra, *J. Phys. Chem. C* 2010, **114**, 15924. b) N.Vilar-Vidal, J. Rivas, M. A. López-Quintela *ACS Catal.* 2012, **2,** 1693.

[2] Y. Xu, X. Yang, S. Zhu, Y. Dou *Colloids and Surfaces A: Physicochem. Eng. Aspects* 2014,**450**, 115.

[3] H. Ding, Ch. Liang , K. Sun , H. Wang , J.K. Hiltunen, Z. Chen, J. Shen *Biosensors and Bioelectronics* 2014, **59**, 216.

[4] L. Shang, S. Dong *J. Mater. Chem.,* 2008, **18**, 4636.

[5] G. Lan, C.-C. Huang, H.-T. Chang *Chem. Commun*. 010, **46,** 21257.

[6] R. Gui , H. Jin *Analyst* 2013, **138,** 7197.

[7] J. Liu, X. Ren, X. Meng, Z. Fang, F. Tang *Nanoscale,* 2013, **5**, 10022–10028

[8] J. A. Ho, H. Chang, W.Su *Anal. Chem.* 2012, **84**, 3246.

[9] J. Xie, Y. Zheng, J. Y. Ying *Chem. Commun*., 2010, **46**, 961–963

[10] B. Adhikari , A. Banerjee *Chem. Mater.,* 2010, **22**, 4364.

[11] D. Hu, Z. Sheng, P. Gong, P. Zhang, L. Cai *Analyst,* 2010, **135**, 1411.

[12] H. Wei, Z. Wang, L. Yang, S. Tian, C. Hou, Y. Lu *Analyst,* 2010, **135**, 1406–1410

[13] C.Huang, Z. Yang, K.Lee, H.Chang *Angew. Chem.* 2007, **119**, 6948.

[14] N. Goswami, A.Giri, M. S. Bootharaju, P.Lourdu Xavier, T. Pradeep, S. Kumar Pal *Anal. Chem.* 2011, **83**, 9676.
[15] Z. Yuan, M. Peng, Y. He, E.S. Yeung *Chem. Commun.,* 2011, **47**, 11981.